An enhanced iot-based emotion-aware personalized user interaction framework with lesi using wr-fuzzy and TCGHMEPM

Raviya,

Leturer,Tagore Govt. College of Education

Abstract: Emotion-aware systems enable Personalized User Interaction (PUI) by dynamically adapting responses based on users' emotional states. However, existing systems failed to capture latent emotional states between features, which affected emotion detection accuracy. Hence, this paper proposes an IoT-based emotion-aware PUI framework with Latent Emotional State Identification (LESI) using Weibull Ramp-Fuzzy (WR-Fuzzy) and Tied Covariance Gaussian Hidden Markov Emission Probability Model (TCGHMEPM). Initially, the DREAMER dataset is pre-processed, followed by data augmentation using Generative Adversarial Network (GAN), clustering using Forgy Soergel K-Means (FSK-Means), and feature extraction. Next, from the extracted features, LESI is performed using TCGHMEPM, and feature fusion is done using Multimodal Autoencoder (MA). Based on LESI and the fused features, emotion classification is conducted using Manifold Gated Swim Recurrent Unit (MGSRU), followed by deep explanation using Rényi Sphere SHapley Additive exPlanations (RSSHAP). Finally, PUI is provided using WR-Fuzzy. Therefore, the proposed MGSRU classified emotions with a higher accuracy (98.8745%) than existing techniques.

Keywords: *Personalized User Interaction, Emotions, Internet of Things (IoT), Artificial Intelligence (AI), Latent Emotional State Identification, Human Automated AI System, and Valence-Arousal-Dominance (VAD).*

1. INTRODUCTION

Emotion is a natural mental and physiological response that influences thoughts, behaviors, and social interactions (Alzhrani et al., 2021) (Fan et al., 2024). These responses can be captured through Electroencephalography (EEG) and Electrocardiography (ECG), which record brain and heart activity, respectively, and their combined analysis enhances Emotion Recognition (ER) (Miao et al., 2025). Furthermore, IoT enables intelligent systems to use physiological data (e.g., EEG and ECG signals) (Murhe et al., 2025). This allows real-time emotion detection in healthcare, human-machine interaction, and beyond (Houssein et al., 2022). AI further improves ER by learning from multimodal data to classify emotions with high accuracy (Khare et al., 2024).

Recent advances in Machine Learning (ML) and Deep Learning (DL) allow ER systems to analyze EEG signals (Abgeena & Garg, 2023). These systems can classify emotions, such as valence (positive or negative feelings), arousal (level of excitement), and dominance (sense of control) (Li et al., 2021). These advancements enable PUI systems that adapt content and responses in real time based on an individual's emotional state (Chin et al., 2021) (Khan et al., 2021). However, existing approaches often overlook latent emotional states (hidden emotions not directly observable) between features, reducing classification accuracy. The motivation of this work is to propose an IoT-based, emotion-aware PUI framework with LESI using WR-Fuzzy and TCGHMEPM to effectively capture nuanced emotional states and enhance personalized interactions.

1.1 Problem Statements

The drawbacks of the traditional approaches are as follows,

- None of the existing systems captured latent emotional states across EEG and ECG features, which reduced ER accuracy.
- In (Dhara et al., 2024), the differences in EEG patterns and ECG signals across age and gender were not considered, limiting the accurate emotion prediction.

- PUIs based on the corresponding emotions were not addressed in (Tuncer et al., 2022), reducing the system's effectiveness in real-time adaptation.
- Most of the existing systems lacked explainability, which reduced trust and personalization of the emotion-aware PUI system.

1.2 Objectives

The objectives of the proposed work are outlined below,

- TCGHMEPM is utilized to perform LESI, thereby improving detection accuracy during emotion classification.
- To predict emotions accurately, FSK-Means is employed for performing the age and gender-based clustering.
- WR-Fuzzy is employed to enable PUI, thereby enhancing the system's effectiveness.
- Deep explanation is provided using RSSHAP, which increases trust in the interaction system.

The structure of this paper is as follows: Section 2 presents the literature survey, Section 3 describes the proposed methodology, Section 4 provides results and discussion, and Section 5 concludes the paper with future recommendations.

2. LITERATURE SURVEY

(Dhara et al., 2024) presented a fuzzy ensemble-based DL model for EEG-based ER. The model extracted signal features and classified them using a fuzzy ensemble-based DL method. Hence, it attained 91.65% accuracy in arousal classification. Yet, the model treated all EEG and ECG signals the same without differentiation, limiting the accurate prediction of emotions.

(Tuncer et al., 2022) established an automated ER system using EEG signals. A multilevel fused feature generation network extracted features, which were classified using a Support Vector Machine (SVM). The model achieved 92.86% accuracy in dominance classification. However, it lacked PUI for the corresponding classified emotions, limiting interpretability and user engagement.

(Liew et al., 2021) developed an explainable ER model using ensembles. Here, clustering using fuzzy adaptive resonance theory, classification using boosted decision tree, and explainability using Shapley Additive Explanations (SHAP) were performed. Hence, the model efficiently recognized the emotions. Nevertheless, it had struggled with training data sensitivity, which affected the stability of clustering.

(Ju et al., 2024) implemented an EEG-based ER model. The model utilized a temporal-difference minimizing neural network to recognize the emotions. Further, maximum mean discrepancy was used to evaluate the difference in features. Therefore, the model attained high precision. But, it faced instability and poor convergence, which reduced training effectiveness.

(Kim et al., 2021) deployed a DL framework for ER. Initially, the signals were pre-processed, and emotions were then classified using Long Short-Term Memory (LSTM). The model attained 81% accuracy in classification. However, the model was affected by noise and artifacts, which reduced the accuracy of ER.

3. PROPOSED FRAMEWORK FOR IoT-BASED EMOTION-AWARE PERSONALIZED USER INTERACTION

This section illustrates an IoT-based emotion-aware PUI framework with LESI, as shown in Figure 1.

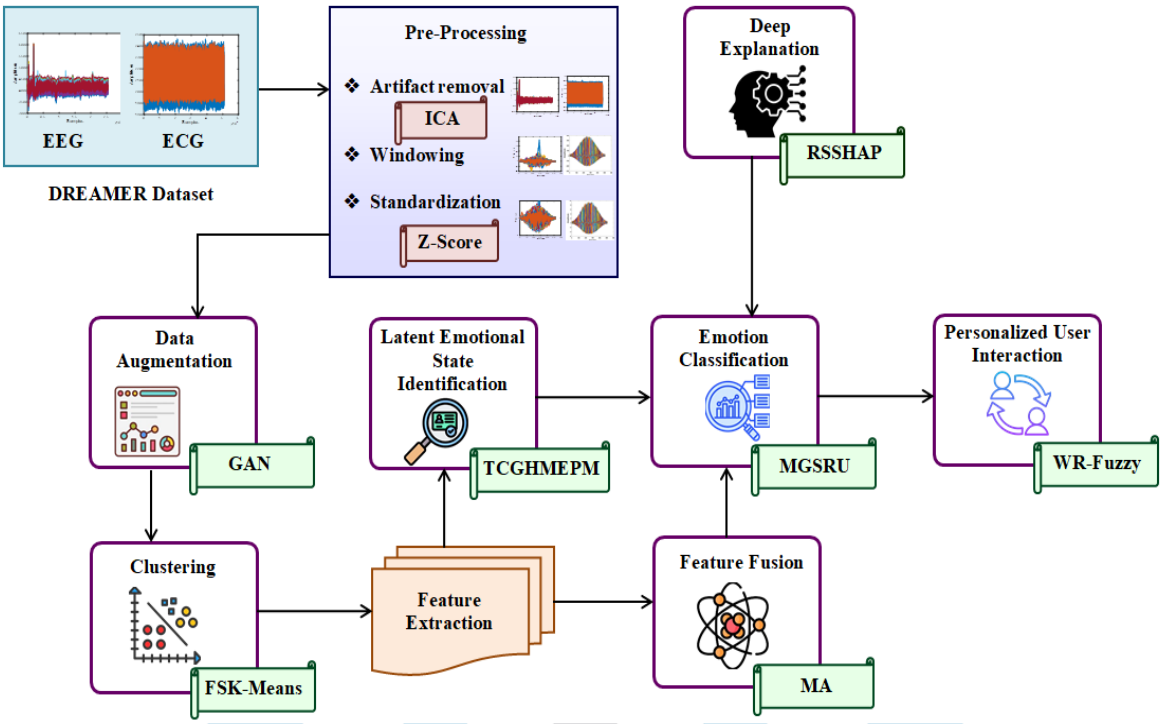

Figure 1: Pictorial Representation for IoT-based Emotion-aware PUI Framework

3.1 DREAMER Dataset

Initially, the DREAMER dataset (D^{dr}) is collected, which contains input signals like EEG (Y^{EEG}) and ECG (Y^{ECG}).

$$D^{dr} = \{\mathrm{Y}^{EEG}, \mathrm{Y}^{ECG}\} \tag{1}$$

These signals are recorded from multiple participants.

3.2 Pre-Processing

Next, to enhance signal quality, pre-processing of (D^{dr}) is done.

- ***Artifact Removal***

Firstly, the artifacts (eye blinks or muscle contractions) in (D^{dr}) are removed using Independent Component Analysis (ICA). ICA separates mixed signals into independent components, enabling the efficient removal of artifacts.

Primarily, (D^{dr}) is centered by subtracting the mean (μ) and then whitened (W) to decorrelate the data.

$$W = \eta(D^{dr} - \mu) \tag{2}$$

Where, (η) depicts the whitening matrix. Next, the independent components (I) are extracted from (W) using a separating matrix (κ), followed by artifact-removed signal (A^{art}) reconstruction.

$$\mathrm{I} = \kappa * W \tag{3}$$

$$\mathrm{A}^{art} = \kappa^{-1} * \mathrm{I} \tag{4}$$

Hence, artifacts are removed from (D^{dr}).

- ***Windowing***

Next, windowing is performed on (A^{art}) based on the time domain to segment it into smaller frames (A'), preserving temporal information for efficient feature extraction.

- ***Standardization***

Now, (A') is standardized using a Z-Score, which scales the signal to zero mean (μ') and unit variance (V) to provide a normalized signal.

$$\wp = \frac{\mathrm{A}' - \mu'}{V} \tag{5}$$

Where, $(\wp)$ indicates the standardized signal (i.e., EEG and ECG signals).

3.3 Data Augmentation

Here, $(\wp)$ are augmented using GAN to increase the dataset size. GAN generates realistic synthetic samples, expanding the dataset.

Primarily, a random noise (n) is fed into the generator (F^{gen}) to produce synthetic data (χ).

$$\chi = F^{gen}(n) \tag{6}$$

Then, the discriminator (F^{dis}) evaluates the real $(\wp)$ and generated (χ) samples to distinguish between them. Next, the GAN is trained iteratively using the discriminator (F^{dloss}) and generator losses (F^{gloss}).

$$F^{dloss} = -\varepsilon_{\wp}\left[\log F^{dis}(\wp)\right] - \varepsilon_{n}\left[\log\left(1 - F^{dis}\left(F^{gen}(n)\right)\right)\right] \tag{7}$$

$$F^{gloss} = -\varepsilon_{n}\left[\log F^{dis}\left(F^{gen}(n)\right)\right] \tag{8}$$

$$\beta = \wp \cup \chi \tag{9}$$

Where, (ε) denotes the expectation operator. Finally, after training, the augmented data (β) are obtained.

3.4 Clustering

Next, (β) is clustered based on age and gender to improve the accuracy of emotion prediction. K-Means assigns all data points to clusters, ensuring uniform distribution. However, it struggles when clusters have varying densities. Therefore, Soergel Distance (SD) is utilized to measure similarity. Also, to overcome (K)-randomness in cluster initialization, Forgy Initialization (FI) is employed, which selects initial cluster centroids randomly from the dataset.

Initially, FI (U) is utilized to initialize (K) cluster centroids (Q) based on (β).

$$U \rightarrow Q = \left\{Q^{1}, Q^{2}, Q^{3}, \cdots\cdots\cdots, Q^{\mathrm{K}}\right\} \tag{10}$$

Next, the SD $\left(\vartheta^{dis}(\beta', \beta'')\right)$ is computed to determine similarity between two points (β') and (β'') from (β).

$$\vartheta^{dis}(\beta', \beta'') = \frac{\sum|\beta' - \beta''|}{\sum \max(\beta', \beta'')} \tag{11}$$

Moreover, based on $\left(\vartheta^{dis}\left(\beta', \beta''\right)\right)$, each data point is assigned (R) to the nearest centroid, and centroids are iteratively updated until convergence, forming final clusters (C).

$$C = \frac{1}{|C|}\sum_{R \in C} R \tag{12}$$

Thus, based on age and gender, (β) are clustered.

3.5 Feature Extraction

From (C), the EEG features $\left(\mathrm{B}^{feat}\right)$, such as theta, alpha, and beta Power Spectral Density (PSD) for each electrode, are extracted. Also, from (C), the ECG features $\left(\hat{\mathrm{B}}^{feat}\right)$ like mean, standard deviation, median, min, max, range of each PQRST complex (P-wave, QRS complex, and T-wave), the root mean square of successive differences between consecutive RR intervals (R-peaks), PSD for Low Frequency (LF) and High Frequency (HF), LF to HF ratio, and total power are extracted.

3.6 Latent Emotional State Identification

Now, LESI is performed using TCGHMEPM to capture latent emotional states between $\left(\mathrm{B}^{feat}\right)$ and $\left(\hat{\mathrm{B}}^{feat}\right)$, enhancing prediction accuracy. A Hidden Markov Model (HMM) captures temporal dependencies within signals and is robust to variations. But, it may require windowing that can distort the signal and does not explicitly account for the time spent in a specific state. Therefore, Tied Covariance Gaussian Emission Probability (TCGEP) is used, which shares covariance across states to improve stability and accurately model state durations.

- ✓ Initially, the hidden emotional states (ζ), the initial probability (ζ_{in}), and the transition probability (ζ_{tra}) are defined. Similarly, observed feature vectors $\left(\zeta^{ob}\right)(\left(\mathrm{B}^{feat}\right)$ and $\left(\hat{\mathrm{B}}^{feat}\right))$ are also defined.
- ✓ Then, TCGEP (T) is applied to improve the stability of the model.

$$\mathrm{T} = \frac{1}{(2\pi)^{q/2}|\gamma|^{1/2}} \exp\left(-\frac{1}{2}\left(\left(\zeta^{ob}\right)-\lambda\right)^{t}\gamma^{-1}\left(\left(\zeta^{ob}\right)-\lambda\right)\right) \tag{13}$$

Where, $(q, \gamma, \lambda, \pi)$ denote the feature dimension, shared covariance across states, mean vector, and mathematical constant of $\left(\mathrm{B}^{feat}\right)$ and $\left(\hat{\mathrm{B}}^{feat}\right)$, respectively, and (t) implies transpose function.

- ✓ Next, based on (ζ_{in}), (ζ_{tra}), and (T), the maximum probability $\left(\tilde{\Xi}\right)$ in $\left(\zeta^{ob}\right)$ is evaluated using the Viterbi algorithm.

$$\tilde{\Xi} = \max_{\zeta}\left[\zeta_{j-1} * \zeta_{in}\right] \times \left(\zeta^{ob}\right)\left(\zeta_{tra}\right) \times \mathrm{T} \tag{14}$$

Where, $\left(\zeta_{j-1}\right)$ signifies the previous (ζ). Finally, regarding $\left(\tilde{\Xi}\right)$ and $\left(\zeta^{ob}\right)$, the latent emotional states are identified. Therefore, by considering the time dependence, the LESI outcome (Ψ) is obtained.

3.7 Feature Fusion

Meanwhile, $\left(\mathrm{B}^{feat}\right)$ and $\left(\hat{\mathrm{B}}^{feat}\right)$ are fused using MA to combine information over time and smooth variations for improved analysis. MA learns compact representations of ECG and EEG features, reducing dimensionality and merging them into a common space.

Primarily, the encoder (Z) compresses $\left(\mathrm{B}^{feat}\right)$ and $\left(\hat{\mathrm{B}}^{feat}\right)$ into compact and meaningful latent representations.

$$Z = encoding\left[\mathrm{B}^{feat}, \hat{\mathrm{B}}^{feat}\right] \tag{15}$$

Next, (Z) is aligned in a common latent space to enable effective feature fusion.

$$P^{fus} = \Gamma_{fusion}(Z) \tag{16}$$

Where, (P^{fus}) indicates fused features, and (Γ_{fusion}) implies the fusion layer operation. Further, if necessary, then the final fused features (Ω) are decoded and reconstructed.

3.8 Emotion Classification

Moreover, based on (Ψ) and (Ω), emotion classification is performed using MGSRU to provide personalized interaction. Gated Recurrent Units (GRUs) excel at capturing temporal dependencies and identifying patterns. However, when applied to small datasets, they tend to overfit. Hence, Manifold Regularization (MR) is utilized to promote sparsity by encouraging many parameters to be zero, thereby avoiding overfitting. Similarly, GRU has vanishing gradient issues that occur during backpropagation. So, the Swin Activation Function (SAF) is employed, which stabilizes gradient flow. Figure 2 depicts the diagrammatic representation of the proposed MGSRU.

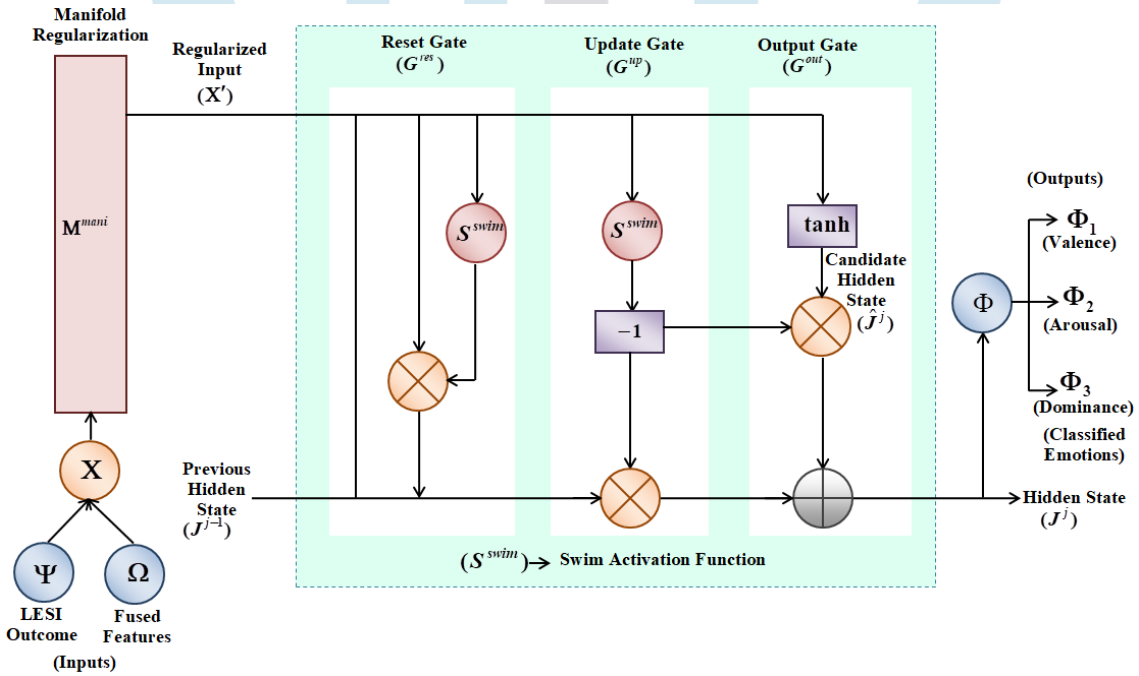

Figure 2: Diagrammatic Representation of MGSRU in Emotion Classification

- Primarily, (Ψ) and (Ω), commonly denoted as (X), are fed into the proposed MGSRU.
- Then, the overfitting issues are mitigated by regularizing (X) using MR (M^{mani}), attaining regularized input (X').

$$\mathrm{M}^{mani} \rightarrow \mathrm{X}' = \frac{1}{(a)^2}\sum_{u,v=1}^{a} \varpi^{uv}\left(g\left(\mathrm{X}^{u}\right) - g\left(\mathrm{X}^{v}\right)\right)^2 \tag{17}$$

Where, (a) signifies the total number of data points, (u,v) represent the indexes of (a), (ϖ) depicts the weight factor, and (g) indicates the MR function.

- Next, the reset gate (G^{res}) and update gate (G^{up}) are computed. Here, SAF (S^{swim}) is utilized to overcome the vanishing gradient problem.

$$G^{res} = S^{swim}\left(r * \left[J^{j-1}, \mathrm{X}'\right] + s\right) \tag{18}$$

$$G^{up} = S^{swim}\left(1 - r' * \left[J^{j-1}, \mathrm{X}'\right] + s'\right) \tag{19}$$

$$S^{swim} = \mathrm{X}' * \frac{1}{2}\left(1 + \frac{d\mathrm{X}'}{\sqrt{1+\mathrm{X}'^{2}}}\right) \tag{20}$$

Here, (r, r') and (s, s') indicate the weights and bias of (G^{res}) and (G^{up}), correspondingly, (J^{j-1}) signifies the previous hidden state at time $(j-1)$, and (d) implies the trainable parameter.

- Now, the candidate hidden state $(\hat{J}^{j})$ is computed, which determines what new information to be added to the hidden state (J^{j}).

$$\hat{J}^{j} = \tanh\left(r'' * \left[G^{up} \otimes J^{j-1}, \mathrm{X}'\right] + s''\right) \tag{21}$$

$$\tanh = \frac{e^{\mathrm{X}'} - e^{-\mathrm{X}'}}{e^{\mathrm{X}'} + e^{-\mathrm{X}'}} \tag{22}$$

$$J^{j} = \left(1 - G^{up}\right) \otimes J^{j-1} + G^{up} \otimes \hat{J}^{j} \tag{23}$$

Where, (r'', s'') represent the weight and bias of $(\hat{J}^{j})$, respectively, (e) demonstrates the exponential function, and $(\tanh)$ depicts the hyperbolic tangent activation function.

- Finally, the output gate (G^{out}) is established to control information flow from $(\hat{J}^{j})$ to the final output.

$$G^{out} = \left[e^{G^{out}} \Big/ \sum e^{G^{out}}\right] * S^{swim}\left(r''' * J^{j} + s'''\right) \tag{24}$$

$$\Phi = \begin{cases} \Phi_1 \rightarrow Valence \\ \Phi_2 \rightarrow Arousal \\ \Phi_3 \rightarrow Dominance \end{cases} \tag{25}$$

Where, (r''', s''') signify the weight and bias of (G^{out}), respectively. Then, from (G^{out}), the classified emotions (Φ) like Valence (Φ_1), Arousal (Φ_2), or Dominance (Φ_3) are obtained.

Pseudocode for MGSRU

Input: LESI Outcome (Ψ) and Fused Features $(\Omega) \rightarrow \mathrm{X}$

Output: Classified Emotions (Φ)

Begin

Initialize (a), (u, v), iteration (Γ), and maximum iteration $(\Gamma^{\max})$

Set $(\Gamma = 1)$

While $(\Gamma \le \Gamma^{\max})$

For each (Ψ) and $(\Omega) \rightarrow \mathrm{X}$ do

Perform MR (M^{mani})

$$\mathrm{M}^{mani} = \frac{1}{(a)^{2}} \sum_{u,v=1}^{a} \varpi^{uv}\left(g\left(\mathrm{X}^{u}\right) - g\left(\mathrm{X}^{v}\right)\right)^{2}$$

Compute (G^{res}) and (G^{res})

Apply $S^{swim} = X' * \frac{1}{2}\left(1 + \frac{dX'}{\sqrt{1+X'^2}}\right)$

Evaluate $\left(\hat{J}^{j}\right)$

Determine $\left(J^{j}\right)$

Compute $\left(G^{out}\right)$

$$G^{out} = \left[e^{G^{out}} \Big/ \sum e^{G^{out}} \right] * S^{swim}\left(r''' * J^{j} + s'''\right)$$

End for

End while

Return (Φ)

End

Thus, the proposed MGSRU accurately classifies the emotions.

3.9 Deep Explanation

Further, to provide a deep explanation about (Φ), RSSHAP is utilized, providing interpretable insights and trust in model decisions. SHAP provides better consistency across model types and improves trust and transparency. However, it is sensitive to weight assignment when improper weight assignment functions are used. Therefore, Rényi Sphere Entropy (RSE) is utilized to assign appropriate weights to the features.

- ✓ Primarily, the features or SHAP values (ξ) are derived from (Φ), followed by weight assignment using the RSE $(\Re)$.

$$\xi = \frac{1}{|h|!}\left(\frac{\left|\Phi^{bin}\right|!\left(h - \left|\Phi^{bin}\right| - 1\right)!}{\left(\Phi\left(\Phi^{bin}\right) - \Phi\left(\Phi^{bin}\right)_h\right)^{-1}} \right) \tag{26}$$

$$\Re(\xi) = \frac{1}{1-k}\log\left(\frac{1}{p^{k}} \sum_{b=1}^{p}\sum_{b'=1}^{p} \mathrm{H}_{\sigma}\left(\left\| \Phi^{b} - \Phi^{b'} \right\|^{k-1} \right) \right) \tag{27}$$

Where, $\left(\Phi^{bin}, h\right)$ indicate the subset and maximum number of (Φ), respectively, $\left(\Phi^{b}, \Phi^{b'}\right)$ illustrate $\left(b^{th}\right)$ and $\left(b'^{th}\right)$ SHAP features, respectively, and $\left(k, p, \mathrm{H}_{\sigma}\right)$ imply the Rényi order, number of samples, and sphere kernel function, respectively.

- ✓ Further, based on $(\Re)$ and base value $\left(\Phi_{base}\right)$, the explanation model (E) is established.

$$\mathrm{E} = \Phi^{base} + \sum_{h'=1}^{h} [\Re]_{h'} \left(\Phi^{bin}\right)_{h'} \tag{28}$$

Here, (h') depicts the index of (h). Thus, RSSHAP provides a deep explanation of why the emotion classification is made.

3.10 Personalized User Interaction

Here, for (Φ), PUI is provided using WR-Fuzzy to give adaptive responses based on the user's emotional state, enhancing the system's effectiveness. Fuzzy is simple and interpretable and can offer effective solutions to complex problems. However, it requires careful tuning of membership functions, scaling factors, and control rules. Therefore, the Weibull Ramp Membership Function (WRMF) is used for precise and adaptive fuzzy reasoning.

Fuzzification: Firstly, the crisp inputs ((Φ)) are converted into fuzzy data $\left(\mathrm{N}^{fuz}\right)$ using WRMF $\left(L^{wei}\right)$.

$$\mathrm{N}^{fuz} = L^{wei} * \Phi \tag{29}$$

$$L^{wei} = \begin{cases} 0, & \Phi \le y \\ 1 - e^{-\left(\frac{\Phi - y}{z}\right)^{o}}, & y < \Phi < z'' \\ 1, & \Phi \ge z'' \end{cases} \tag{30}$$

Where, (z, o) indicate the Weibull parameters, and (y, z'') illustrate the start and saturation point of membership, respectively.

Rule Generation: Next, based on (N^{fuz}) and (Φ), the fuzzy rules (O^{rules}) are generated to provide the PUI.

$$\mathrm{O}^{rules} = \begin{cases} if \ \ \Phi_1 \ \ is \ obtained, \ then \ \ provide \ C^{pl} \\ if \ \ \Phi_2 \ \ is \ obtained, \ then \ \ provide \ C^{su} \\ if \ \ \Phi_3 \ \ is \ obtained, \ then \ \ provide \ C^{fr} \end{cases} \tag{31}$$

Where, (C^{pl}) indicates interactions like playing calming, uplifting music, reading motivational quotes, and watching a fish tank, (C^{su}) implies interactions like walking, stretching, swimming, and motivational fitness, and (C^{fr}) represents interactions like engaging with friends, attending functions, interacting with professionals, and reading books.

Defuzzification: Further, the defuzzification converts the data into a crisp value (N^{def}) (PUI) through inferred outcome $(\mathrm{N}^{\inf})$ computation.

$$\mathrm{N}^{def} = \frac{\sum \mathrm{N}^{\inf} \times L^{wei}\left(\mathrm{N}^{\inf}\right)}{\sum L^{wei}\left(\mathrm{N}^{\inf}\right)} \tag{32}$$

Therefore, (N^{def}) determines the PUI for the users based on their emotions.

Pseudocode for WR-Fuzzy

Input: Classified Emotions (Φ)
Output: PUI (N^{def})

Begin
  Initialize (z, o), (y, z''), iteration (Γ), and maximum iteration $(\Gamma^{\max})$
  Set $(\Gamma = 1)$
  While $(\Gamma \le \Gamma^{\max})$
    For each (Φ) do
      Perform fuzzification
        $\mathrm{N}^{fuz} = L^{wei} * \Phi$
      Apply WRMF (L^{wei})
      Generate rules (O^{rules})
      Infer data # $(\mathrm{N}^{\inf})$
      Perform defuzzification
        $\mathrm{N}^{def} = \frac{\sum \mathrm{N}^{\inf} \times L^{wei}\left(\mathrm{N}^{\inf}\right)}{\sum L^{wei}\left(\mathrm{N}^{\inf}\right)}$
    End for
  End while
  Return (N^{def})

End

Hence, the proposed framework efficiently supports user interactions for the classified emotions, and its performance analysis is discussed further.

4. RESULT AND DISCUSSION

In this section, the performance of the proposed framework is evaluated. The implementation of the proposed work is carried out on the Python platform.

4.1 Dataset Description

The proposed work uses the DREAMER dataset to identify emotions, which includes 23 participants (14 male and 9 female) and 18 videos. A summary of the dataset is presented in Table 1.

Table 1: DREAMER Dataset Details

Dataset	Classes	Before Augmentation	After Augmentation
DREAMER	Valence	414	2070
	Arousal		
	Dominance		

From the entire dataset (2070), 80% (1656) and 20% (414) of the data are used for training and testing, respectively.

Table 2: Image Results

Classes/ Phases	Valence	Arousal	Dominance
	EEG		
Input Signal	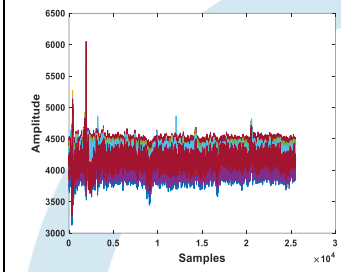	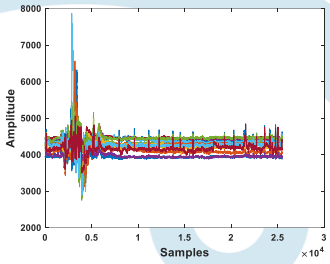	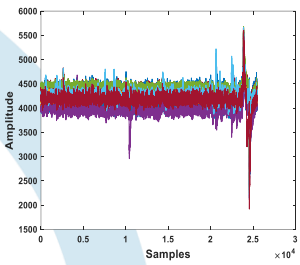
Artifact Removal	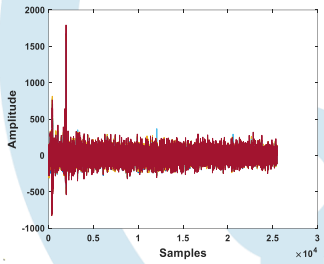	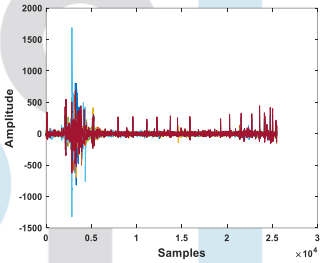	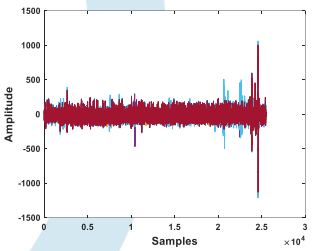
Windowing	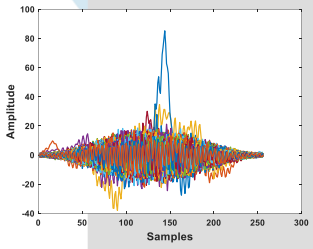	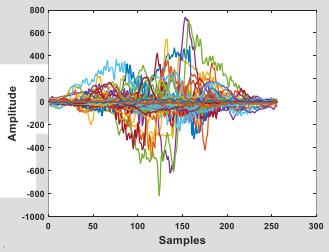	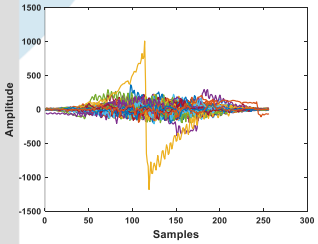
Standardization	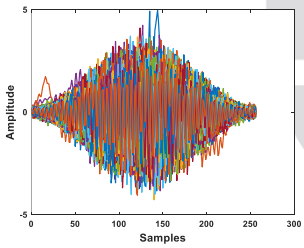	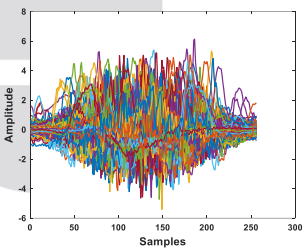	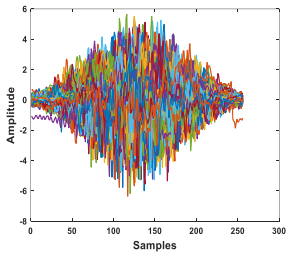
	ECG		
Input Signal	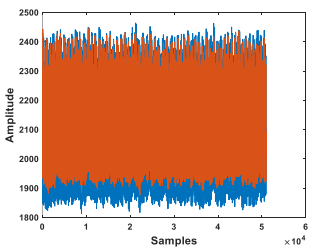	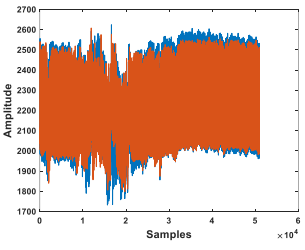	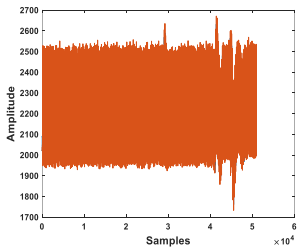

Artifact Removal	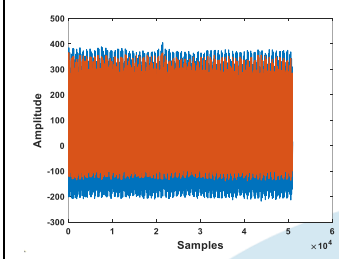	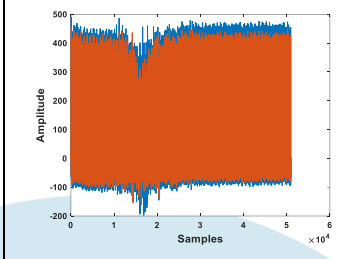	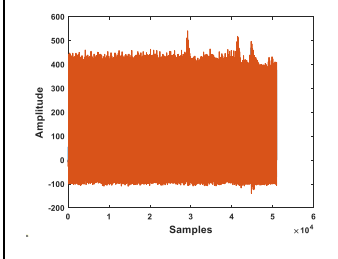
Windowing	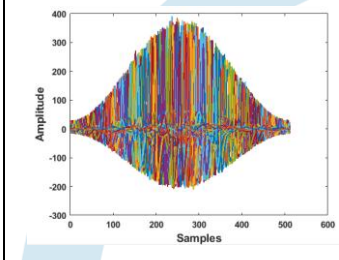	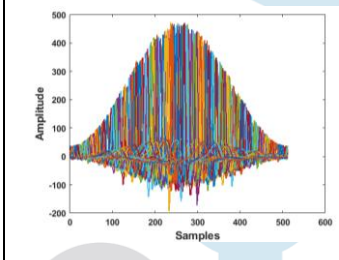	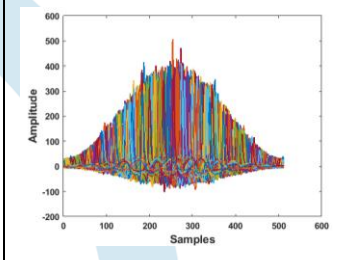
Standardization	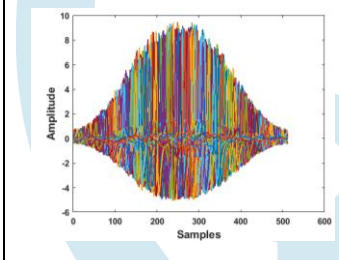	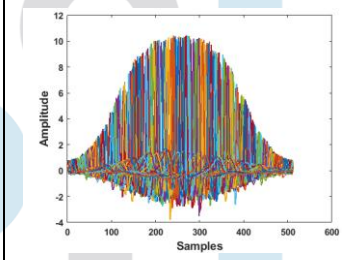	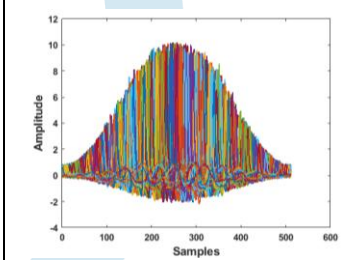

Table 2 depicts the image results of the EEG and ECG signals.

4.2 Performance Analysis

Here, the performance of the proposed methods is compared with the existing methods.

Table 3: Analysis of TCGHMEPM in LESI

Techniques	SE (%)	Perplexity	BS
Proposed TCGHMEPM	4.1054	9.1028	0.2206
HMM	12.5645	17.2369	0.4121
GMM	28.5678	24.1478	0.6655
DBN	33.2104	33.2065	0.8059
CRF	37.8475	36.3284	0.9083

As shown in Table 3, the proposed TCGHMEPM achieved lower Sequence Error (SE), perplexity, and Brier Score (BS) of 4.1054%, 9.1028, and 0.2206, respectively. In contrast, the existing HMM, Gaussian Mixture Model (GMM), Dynamic Bayesian Network (DBN), and Conditional Random Fields (CRF) attained higher SE, perplexity, and BS values. For instance, the existing HMM attained a higher SE (12.5645), perplexity (17.2369), and BS (0.4121). Hence, by utilizing TCGEP, the proposed TCGHMEPM efficiently identified latent emotional states.

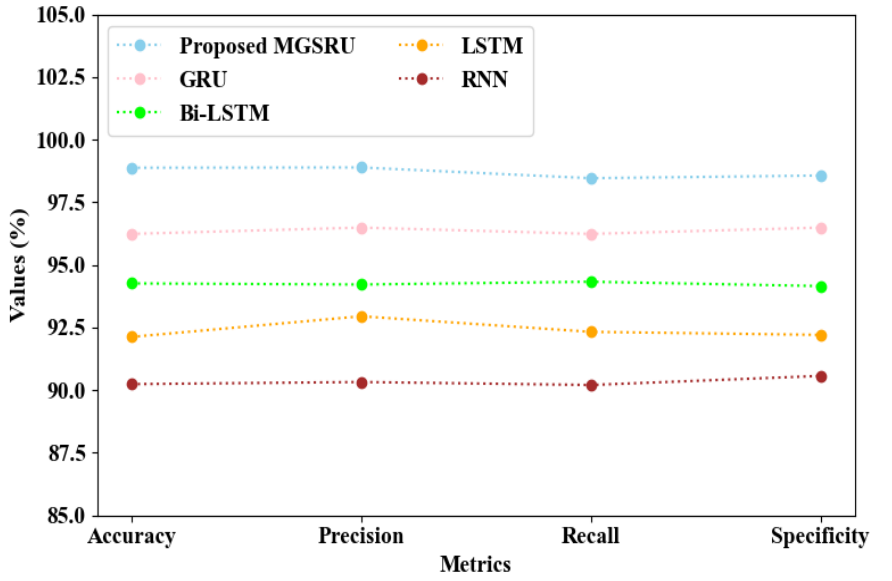

(a)

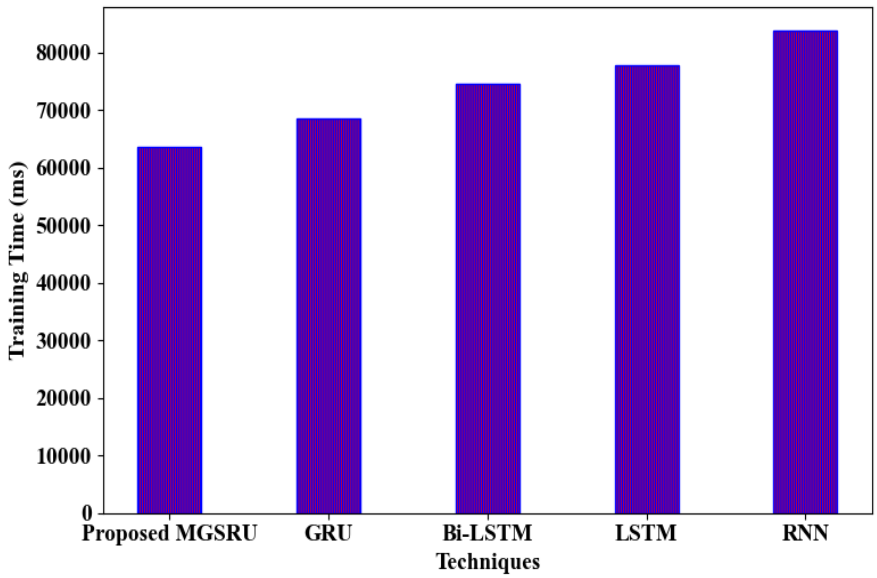

(b)

Figure 3 (a) and (b): Performance Validation of MGSRU in Emotion Classification

Table 4: Emotion Classification Analysis

Techniques	Accuracy (%)	Precision (%)	Recall (%)	Specificity (%)	Training Time (ms)
Proposed MGSRU	98.8745	98.8865	98.4578	98.5645	63528
GRU	96.2356	96.4875	96.2351	96.4872	68471
Bi-LSTM	94.2598	94.2147	94.3265	94.1528	74545
LSTM	92.1245	92.9481	92.3265	92.2047	77842
RNN	90.2394	90.3251	90.2056	90.5687	83695

The proposed MGSRU outperformed the existing techniques by achieving higher accuracy (98.8745%), precision (98.8865%), recall (98.4578%), and specificity (98.5645%) while also reducing training time

(63528ms), as shown in Figures 3 (a) and (b) and Table 4. This improvement was due to the use of MR and SAF. In contrast, the prevailing GRU, Bi-directional Long Short-Term Memory (Bi-LSTM), LSTM, and Recurrent Neural Network (RNN) showed relatively lower performance, with longer training durations. Hence, the proposed MGSRU classified emotions more accurately and efficiently than the existing techniques.

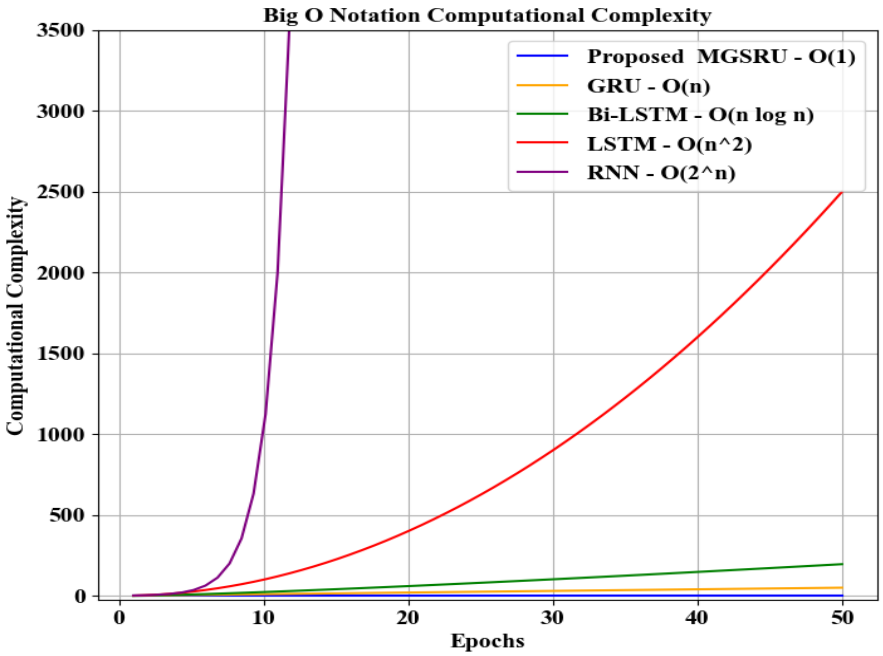

Figure 4: Computational Complexity Assessment

As illustrated in Figure 4, the proposed MGSRU achieved the lowest computational complexity with O(1), demonstrating stable performance across epochs. In contrast, the prevailing GRU (O(n)), Bi-LSTM (O(n log n)), LSTM ($O(n^2)$), and RNN ($O(2^n)$) exhibited significantly higher complexity. Thus, the proposed MGSRU was most efficient in terms of computational cost.

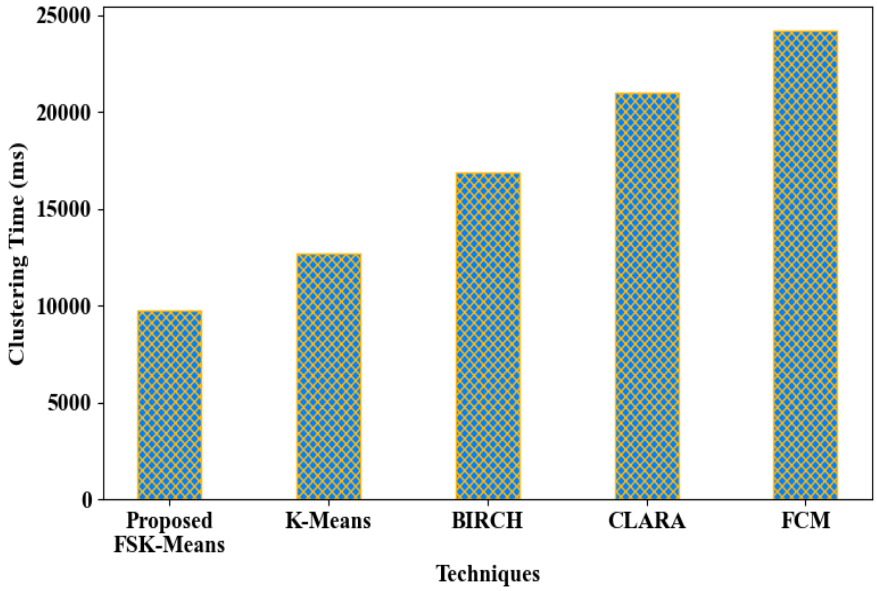

Figure 5: Clustering Time Analysis

Figure 5 shows the clustering time comparison between the proposed FSK-Means and existing techniques. Due to the employment of SD and FI, the proposed FSK-Means had the lowest clustering time of 9745ms, outperforming the conventional K-Means (12656ms), Balanced Iterative Reducing and Clustering using Hierarchies (BIRCH) (16847ms), Clustering Large Applications (CLARA) (20958ms), and Fuzzy C-Means (FCM) (24187ms). Therefore, the proposed FSK-Means delivered more accurate clustering results.

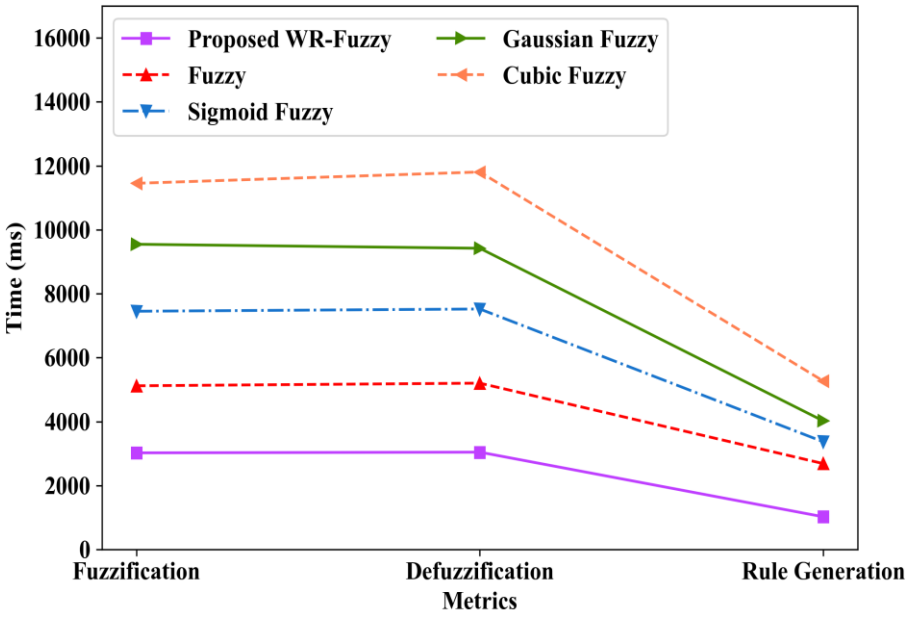

Figure 6: Validation of WR-Fuzzy for PUI

The proposed WR-Fuzzy's performance in PUI is compared with the existing techniques, as shown in Figure 6. The proposed WR-Fuzzy took 3024ms, 3045ms, and 1024ms for fuzzification, defuzzification, and rule generation, respectively. In comparison, the existing Fuzzy, Sigmoid Fuzzy, Gaussian Fuzzy, and Cubic Fuzzy attained higher average fuzzification, defuzzification, and rule generation times of 8393.25ms, 8488.25ms, and 3836.5ms, respectively. Therefore, by employing WRMF, the proposed WR-Fuzzy provided PUI more interactively, enabling the user to receive appropriate interactions effectively.

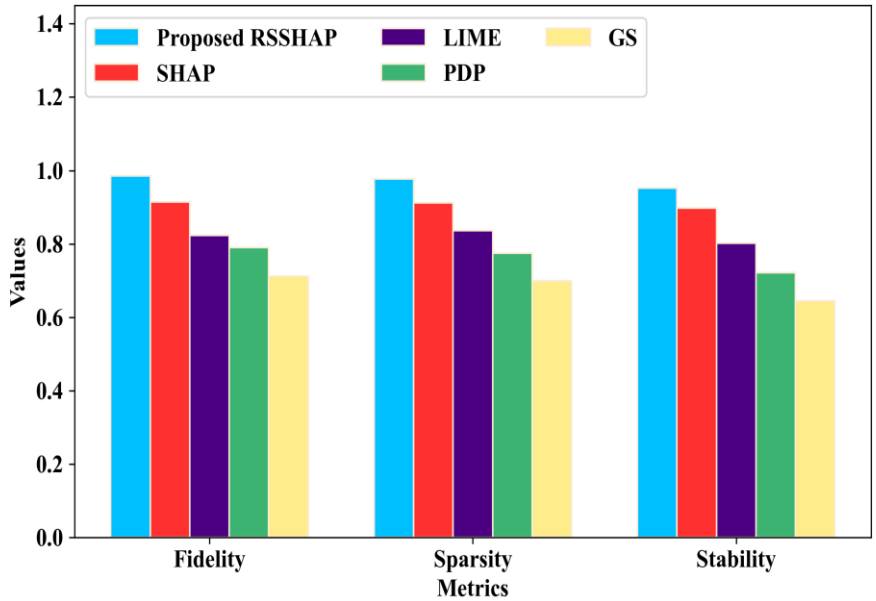

Figure 7: Analysis of RSSHAP for Deep Explanation

Figure 7 shows that by utilizing RSE, the proposed RSSHAP achieved high interpretability with 0.9856 fidelity, 0.9765 sparsity, and 0.9526 stability. In contrast, existing SHAP, Local Interpretable Model-agnostic Explanations (LIME), Partial Dependence Plot (PDP), and Global Surrogate (GS) attained lower fidelity scores of 0.9145, 0.8236, 0.7896, and 0.7124, respectively, and reduced sparsity and stability. Hence, compared to existing methods, the proposed RSSHAP provided more reliable classification explanations.

4.3 Comparative Analysis

Here, the comparative analysis of the proposed and traditional works is depicted.

Table 5: Comparative Assessment of the Proposed and Existing Techniques

References	Techniques/Methods Used	Dataset	Accuracy (%)	Precision (%)
Proposed	MGSRU	DREAMER	98.8745	98.8865
(Nalwaya et al., 2022)	K-nearest neighbors (KNN)	DREAMER	97.87	98.08
(Nita et al., 2021)	Convolutional Neural Network (CNN)	DREAMER	86.0866	-
(Topic et al., 2022)	CNN + SVM	DREAMER	92.2166	-
(Ma et al., 2024)	Dual Attention Mechanism with CNN and Bi-LSTM	DREAMER	88.8766	89.2733
(Kumari et al., 2022)	Emotion-based Capsule Network (EmotionCapsNet)	DREAMER	81.96	-

Table 5 presents the comparative assessment of the proposed MGSRU against traditional methods for emotion classification using the DREAMER dataset. The proposed MGSRU achieved the highest performance with 98.8745% accuracy and 98.8865% precision, surpassing the existing KNN and Dual Attention with CNN and Bi-LSTM. Likewise, lower results were attained by prior (Nita et al., 2021) and (Topic et al., 2022), which employed CNN (86.0866% accuracy) and CNN+SVM (92.2166% accuracy). Similarly, EmotionCapsNet also yielded reduced accuracy (81.96%). These findings demonstrated that the proposed MGSRU effectively addressed the limitations of existing approaches and significantly enhanced the IoT-based emotion-aware PUI.

5. CONCLUSION

This paper presented an enhanced IoT-based emotion-aware PUI framework with LESI using WR-Fuzzy and TCGHMEPM. Initially, EEG and ECG signals from the DREAMER dataset were pre-processed and augmented. Clustering was then performed using FSK-Means with a clustering time of 9745ms. Further, LESI was performed using TCGHMEPM with 9.1028 perplexity. Moreover, based on the fused features and LESI outcomes, emotion classification was performed using MGSRU, achieving 98.8745% accuracy and 98.8865% precision. A deep explanation was provided using RSSHAP, with a 0.9856 fidelity score. Finally, personalized interaction was delivered using WR-Fuzzy, with a rule generation time of 1024ms. Thus, an IoT-based emotion-aware PUI was efficiently developed, thereby enabling seamless user interaction.

Future Recommendation

In the future, the proposed model will be enhanced by incorporating advanced techniques to effectively handle mixed emotions occurring simultaneously, thereby improving the accuracy of recognition.

REFERENCES

- **Dataset Link: https://www.kaggle.com/datasets/phhasian0710/dreamer**
- Abgeena, A., & Garg, S. (2023). EEG evoked automated emotion recognition using deep convolutional neural network. *2023 5th International Conference on Electrical, Computer and Communication Technologies, ICECCT*, 1–8. https://doi.org/10.1109/ICECCT56650.2023.10179711

- Alzhrani, W., Doborjeh, M., Doborjeh, Z., & Kasabov, N. (2021). Emotion Recognition and Understanding Using EEG Data in A Brain-Inspired Spiking Neural Network Architecture. *Proceedings of the International Joint Conference on Neural Networks*, 1–10. https://doi.org/10.1109/IJCNN52387.2021.9533368

- Chin, Z. Y., Zhang, Z., Wang, C., & Ang, K. K. (2021). An Affective Interaction System using Virtual Reality and Brain-Computer Interface. *Proceedings of the Annual International Conference of the IEEE Engineering in Medicine and Biology Society, EMBC*, 6183–6186. https://doi.org/10.1109/EMBC46164.2021.9630045

- Dhara, T., Singh, P. K., & Mahmud, M. (2024). A Fuzzy Ensemble-Based Deep learning Model for EEG-Based Emotion Recognition. *Cognitive Computation, 16*(3), 1364–1378. https://doi.org/10.1007/s12559-023-10171-2

- Fan, Z., Chen, F., Xia, X., & Liu, Y. (2024). EEG Emotion Classification Based on Graph Convolutional Network. *Applied Sciences (Switzerland), 14*(2), 1–18. https://doi.org/10.3390/app14020726

- Houssein, E. H., Hammad, A., & Ali, A. A. (2022). Human emotion recognition from EEG-based brain–computer interface using machine learning: a comprehensive review. *In Neural Computing and Applications, 34*. https://doi.org/10.1007/s00521-022-07292-4

- Ju, X., Li, M., Tian, W., & Hu, D. (2024). EEG-based emotion recognition using a temporal-difference minimizing neural network. *Cognitive Neurodynamics, 18*(2), 405–416. https://doi.org/10.1007/s11571-023-10004-w

- Khan, P., Ranjan, P., & Kumar, S. (2021). AT2GRU: A Human Emotion Recognition Model With Mitigated Device Heterogeneity. *IEEE Transactions on Affective Computing, 14*(2), 1–12. https://doi.org/10.1109/TAFFC.2021.3114123

- Khare, S. K., Blanes-Vidal, V., Nadimi, E. S., & Acharya, U. R. (2024). Emotion recognition and artificial intelligence: A systematic review (2014–2023) and research recommendations. *Information Fusion, 102*, 1–36. https://doi.org/10.1016/j.inffus.2023.102019

- Kim, S., Anh, N., Nguyen, T., Yang, H., & Lee, S. (2021). eRAD-Fe : Emotion Recognition-Assisted Deep Learning Framework. *IEEE Transactions On Instrumentation And Measurement, 70*, 1–12. https://ieeexplore.ieee.org/abstract/document/9547276/

- Kumari, N., Anwar, S., & Bhattacharjee, V. (2022). Time series-dependent feature of EEG signals for improved visually evoked emotion classification using EmotionCapsNet. *Neural Computing and Applications, 34*(16), 13291–13303. https://doi.org/10.1007/s00521-022-06942-x

- Li, C., Zhang, Z., Song, R., Cheng, J., Liu, Y., & Chen, X. (2021). EEG-Based Emotion Recognition via Neural Architecture Search. *IEEE Transactions on Affective Computing*, 1–12. https://doi.org/10.1109/TAFFC.2021.3130387

- Liew, W. S., Loo, C. K., & Wermter, S. (2021). Emotion Recognition Using Explainable Genetically Optimized Fuzzy ART Ensembles. *IEEE Access, 9*, 1–19. https://doi.org/10.1109/ACCESS.2021.3072120

- Ma, Y., Huang, Z., Yang, Y., Zhang, S., Dong, Q., Wang, R., & Hu, L. (2024). Emotion Recognition Model of EEG Signals Based on Double Attention Mechanism. *Brain Sciences, 14*, 1–20. https://doi.org/10.3390/brainsci14121289

- Miao, Y., Wang, H., Wang, W., & Song, L. (2025). DuMoNet: Enhancing Emotion Recognition with a Dual-Modality Structure from EEG and ECG. *International Conference on Digital Signal Processing, DSP*, 1–5. https://doi.org/10.1109/DSP65409.2025.11074850

- Murhe, V., Nagpure, S., Bihade, V., & Bhanudas, D. A. (2025). IoT-ConvNet + LAMB: a deep learning based emotion recognition framework using smart IoT systems. *International Journal of Information Technology (Singapore)*, 1–7. https://doi.org/10.1007/s41870-025-02482-4

- Nalwaya, A., Das, K., & Pachori, R. B. (2022). Automated Emotion Identification Using Fourier–Bessel Domain-Based Entropies. *Entropy*, *24*(10), 1–22. https://doi.org/10.3390/e24101322

- Nita, S., Bitam, S., Heidet, M., & Mellouk, A. (2021). A new data augmentation convolutional neural network for human emotion recognition based on ECG signals. *IEEE Journal Of Biomedical And Health Informatics*, 1–18. https://doi.org/10.1016/j.bspc.2022.103580

- Topic, A., Russo, M., Stella, M., & Saric, M. (2022). Emotion Recognition Using a Reduced Set of EEG Channels Based on Holographic Feature Maps. *Sensors*, *22*(9), 1–25. https://doi.org/10.3390/s22093248

- Tuncer, T., Dogan, S., & Subasi, A. (2022). LEDPatNet19: Automated Emotion Recognition Model based on Nonlinear LED Pattern Feature Extraction Function using EEG Signals. *Cognitive Neurodynamics*, *16*(4), 779–790. https://doi.org/10.1007/s11571-021-09748-0